Proceedings of the Sixth International Conference on
Railway Technology: Research, Development and Maintenance
Edited by: J. Pombo
Civil-Comp Conferences, Volume 7, Paper 15.8
Civil-Comp Press, Edinburgh, United Kingdom, 2024
ISSN: 2753-3239, doi: 10.4203/ccc.7.15.8

New Perspectives on Running Safety in Ballastless Railway Bridges

G. Ferreira, P. A. Montenegro, A. A. Henriques and R. Calçada

CONSTRUCT-LESE, Faculty of Engineering, University of Porto, Portugal

Abstract

Running safety on ballastless bridges is conditioned by the Eurocode EN 1990 A2 on a limit for vertical acceleration. Although it seems this limit is indicative of avoiding the loss of wheel-rail contact, it is unclear whether such accelerations correspond to derailment situations. This communication presents a parametric study of five single-span slab track bridges with varying levels of track quality. Using the High-Speed Load Model A of the EN 1991-2 and a three-dimensional train-track-bridge-interaction approach, deck acceleration and derailment criteria (Nadal and Unloading) are calculated. The results indicate a poor correlation between acceleration and the criteria. It is concluded that track quality is the conditioning factor.

Keywords: ballastless railway bridges, derailment, running safety, deck acceleration, Eurocodes, high-speed railways.

1 Introduction

Like all civil engineering structures in Europe, railway bridges are designed according to the Eurocodes. These norms are not, however, immutable, and are currently under revision [1]. One aspect that has concerned researchers in recent years [2, 3] is the EN

1990 A2 [4] limit for vertical deck acceleration. While the value for ballasted tracks derives from tests commissioned by the European Rail Research Institute [5], the ballastless track limit is likely based on the assumption that a 1 g deck acceleration may imply wheel detachment. Furthermore, the normative values (respectively, 3.5 m/s^2 and 5 m/s^2) are based on a seemingly arbitrary safety factor of 2.0.

The scientific community has devoted resources to the study of ballastless bridges, focusing on topics such as acceleration [6], local deck vibration [7], seismic action [8], and passenger comfort [9]. The present communication focuses the relation between deck acceleration and wheel-rail contact, studying derailment risk with three-dimensional train-track-bridge interaction (TTBI) models. The motivation of this work is to address a) the correspondence between derailment and deck acceleration; b) the indispensability of considering lateral dynamics; and c) the relative importance of track quality compared to vibration in resonance.

2 Methods

The proposed methodology consists in performing a parametric study of 5 single-track slab bridges with spans between 10 m and 30 m, each subjected to a critical load model running at speeds from 140 km/h to 400 km/h. Each simulation takes into account 11 rail irregularities profiles: 1 smooth track, 5 high quality profiles, and 5 lower quality. The metrics registered in each run are the maximum midspan vertical acceleration and the time histories of the lateral Y and vertical Q contact forces for each train wheel, to calculate derailment criteria (Nadal ξ_N and Unloading ξ_U), using:

$$\xi_N = \frac{Y}{Q} \tag{1}$$

$$\xi_U = 1 - \frac{Q}{Q_0} \tag{2}$$

where Q_0 is the static load for each wheel. The normative limits are 3.5 m/s^2 for acceleration a_{lim} [4], 0.8 for Nadal N_{lim} [10], and 0.6 for Unloading U_{lim} [11].

The bridges where modelled after [12], with cross-sections that give accelerations near the limit at around 380 km/h. The finite elements (FE) models where done in ANSYS [13], using Timoshenko beam elements to model the deck, track slab and rails, and spring-dashpots to model the concrete-asphalt mortar bed, subgrade and fastenings. Rayleigh damping matrices are employed with ratios from [14]. Readers are referred to the annexes in [3] for mechanical and geometric properties. A lateral view of the model for the 25 m bridge can be seen in Fig. 1, which displays the first bending mode. In Fig. 2, the 3D view shows how the deck is represented by a beam in its center of gravity, with rigid elements connecting it to the rails.

Regarding the trains, the High-Speed Load Model A (HSLM-A) [14], which is a set of moving point loads, is adapted for this study as 3D FE models of articulated trains, with masses that represent the Eurocode's axle loads [2] and primary and secondary

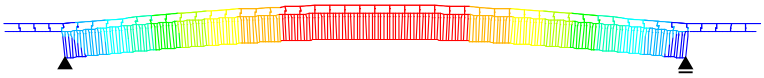

Figure 1: Bending mode of the 25 m bridge FE model (n_0 = 5.44 Hz).

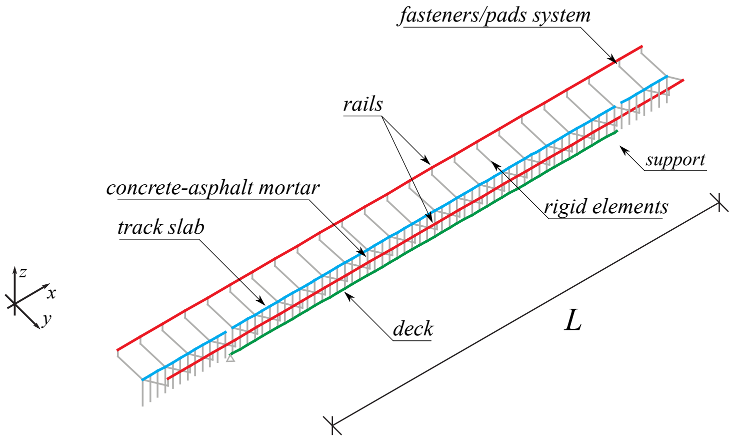

Figure 2: 3D view of the FE model.

suspension characteristics from the literature [15, 16]. The FE model, depicted in Fig. 3, uses beam elements for rigid beams, spring-dampers for the suspensions, and mass elements for localized masses. Spherical joints connect the rigid connections between shared bogies of adjacent carriages.

Each bridge is paired with a critical configuration from the 10 available HSLM-A models. Using a simple moving loads approach, the maximum midspan acceleration a is obtained for every train, as seen in Fig. 4 for the 25 m bridge. The train considered as critical is the one that causes a surpassing of a_{lim} at around 1.2 times the design speed of 320 km/h [14], i.e. circa 380 km/h.

The rail irregularities ζ profiles were generated using the German Power Spectral Density (PSD) functions [17], with a wavelength interval from 3 m to 150 m. The high quality track profiles consider longitudinal and alignment levels compatible with a well-maintained track of the Chinese PSD [18], while the lower quality profiles correspond to the alert limit from [19]. Fig. 5 exemplifies both levels.

The TTBI analyses are done with the numerical tool developed by [20] in MATLAB [21], which uses a custom finite element for the wheel-rail interface. The Y and Q responses are filtered with a low-pass, 4th-order Butterworth filter cut-off at 20 Hz [11].

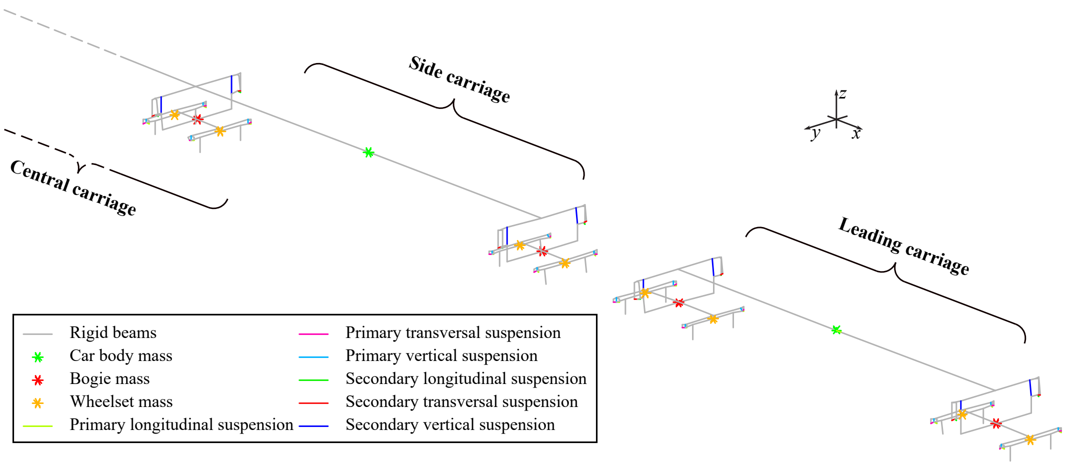

Figure 3: FE model of the train.

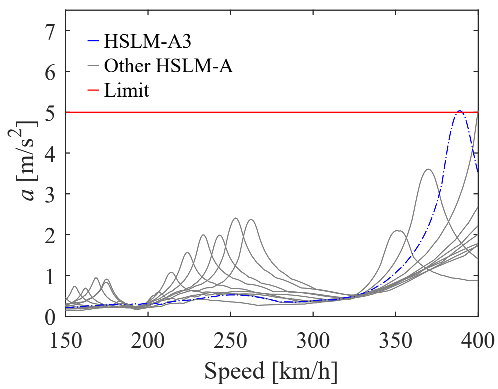

Figure 4: Maximum midspan acceleration for the 25 m bridge with the HSLM-A.

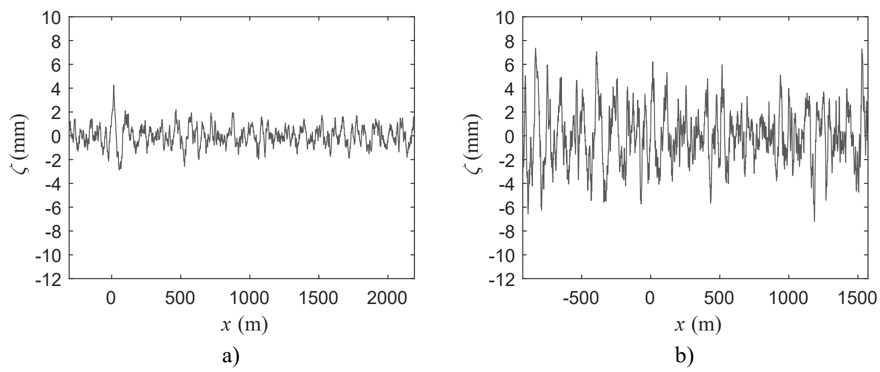

Figure 5: Example realization of track's vertical irregularities: a) well-maintained; b) Alert limit.

3 Results

The envelopes of the maximum values of deck acceleration and of the criteria are shown in Fig. 6. Lines with the results considering smooth tracks are also depicted. Through them, it is clear that the absence of rail irregularities results in near zero ξ_N value, while for ξ_U, that scenario coincides with the lower bound of the envelopes. The a curves for smooth tracks serve as a benchmark for the entire process, given their similarity to the simplified moving loads assessment.

Looking at the envelopes, ξ_U generally increases with speed, with less evident peaks at subharmonic speed values. Conversely, ξ_N is far less affected by resonance, being only affected by track conditions. This is due to the increasing importance of lateral force on each wheel and decreasing vertical forces as irregularities get worse. Even so, the Alert limit irregularities are still notoriously far from producing effects close to N_{lim}.

The results indicate that an assessment based on deck acceleration would result in a negative evaluation (since a_{lim} is surpassed), even though on the same conditions the derailment criteria are never indicative of failure. In fact, the maximum ξ_U calculated is below 0.38 for the higher quality realizations and below 0.48 for lower quality. This observation does not support the thesis of assessing running safety via deck acceleration.

The conclusion is strengthened by using data points with pairs $[a, \xi_N]$ and $[a, \xi_U]$ (represented in Fig. 7) and fitting linear regression models on them. The resulting coefficients of determination (r^2) show that the relation is insufficient to conclude that deck acceleration is an indicator of derailment.

Given the distance of both criteria to the respective limits, it is worth running additional simulations with irregularity levels even worse than the Alert limit. To that end, 5 new profiles were generated where the standard deviation in the 3 m to 25 m wavelength range was increased by 50% ($\sigma_{3-25} \times 1.5$) and another 5 with a 100% increase ($\sigma_{3-25} \times 2$). This set was tested on the 25 m bridge at 390 km/h, which is the clearest scenario with resonance. The resulting values in Fig. 8 have maxima ξ_U of 0.704 and ξ_N of 0.505, on the worst track conditions. It was necessary to double the roughness of the lower track quality to have ξ_U above U_{lim} and ξ_N above 0.5.

Since the bridge vibration seems to have an almost negligible effect on the derailment criteria, the same analyses of the 25 m bridge at 390 km/h where replicated with a rigid bridge instead. The results, represented in Fig. 9, further sustain the observation that track condition controls the performance of the criteria, regardless of the rigidity of the bridge. In fact, the sums of squared differences between both situations is 0.04 for Unloading and 0.01 for Nadal.

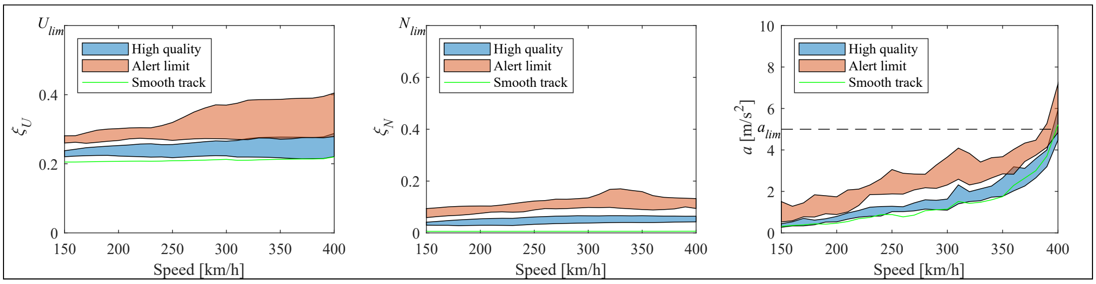

a)

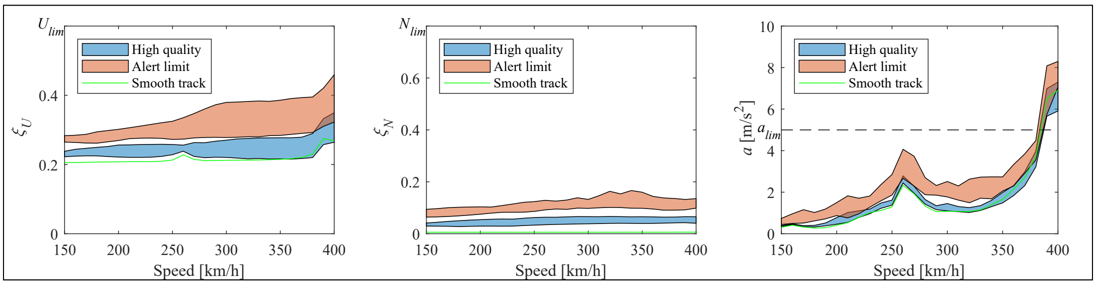

b)

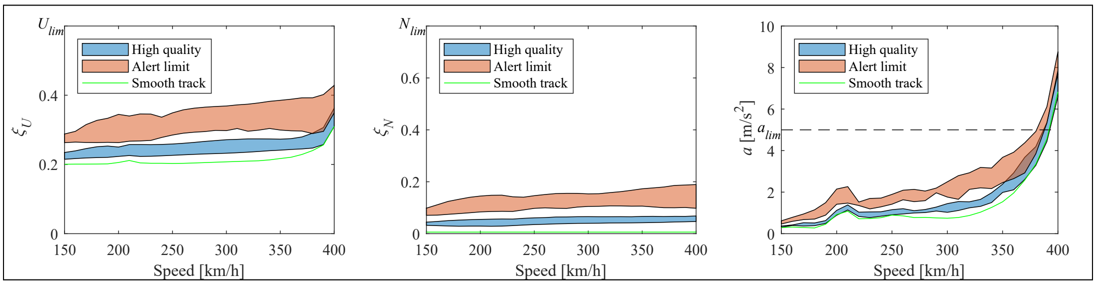

c)

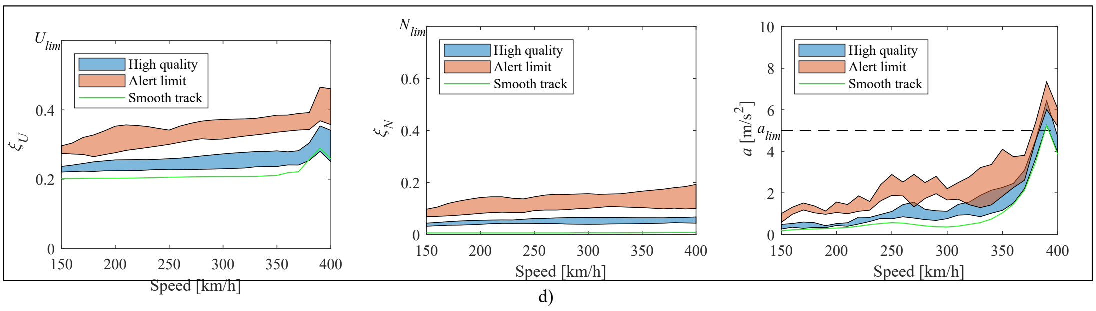

d)

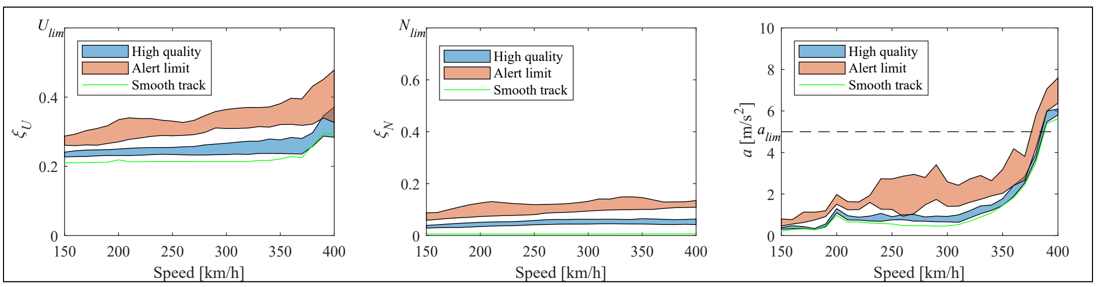

e)

Figure 6: ξ_U, ξ_N and a envelopes. a) 10 m bridge; a) 15 m bridge; a) 20 m bridge; a) 25 m bridge; a) 30 m bridge.

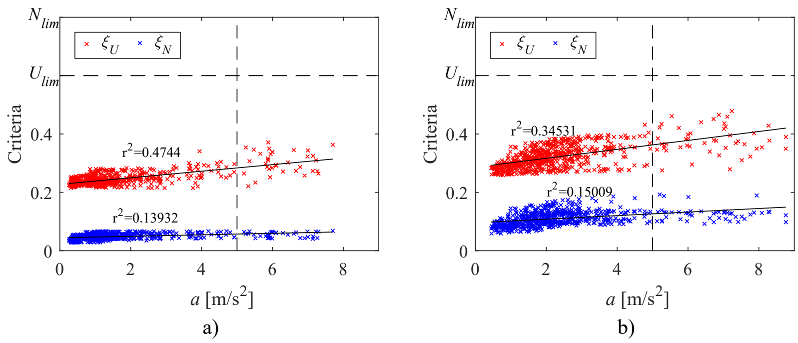

Figure 7: Acceleration and derailment criteria on all bridges at every speed. a) high quality realizations; b) Alert limit realizations.

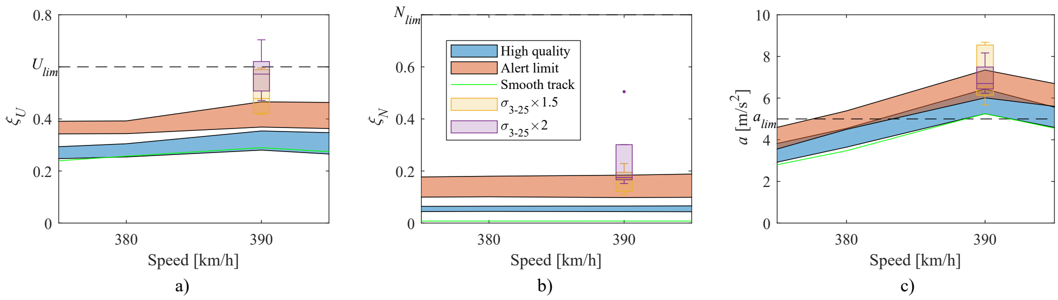

Figure 8: Results with increased irregularities on the 25 m bridge. a) ξ_U; b) ξ_N; c) a.

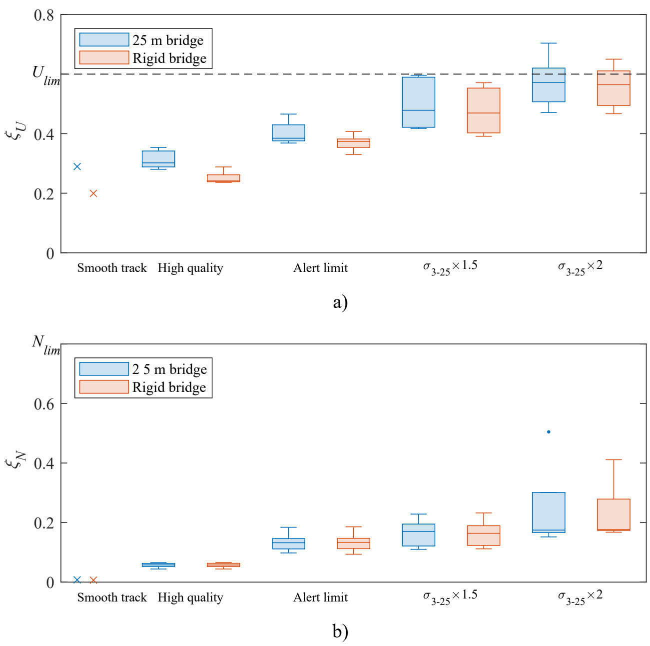

Figure 9: Influence of the bridge vibration. a) ξ_U; b) ξ_N.

4 Conclusions & Contributions

The parametric analyses conducted in this communication question the use of an acceleration limit for running safety evaluation. It is shown that ballastless bridges can show accelerations above 5 m/s^2 without a corresponding derailment criterion being met. The Unloading criterion has a closer relation to acceleration than the Nadal criterion, meaning that vertical dynamics are indispensable for the assessment of running safety. 3D dynamics should not be neglected in the presence of relevant sources of lateral instability. As for the relation with track quality, the Nadal criterion is almost exclusively affected by it, while the Unloading criterion is somewhat more affected by speed. Acceleration is, however, much more telling of resonance. For derailment matters, track quality is the determinant factor.

Acknowledgements

The authors acknowledge the financial support of "InBridge4EU – Enchanded Interfaces and train categories for dynamic compatibility assessment of European railway bridges" (funded by European funds through Horizon Europe, Europe's Rail Joint Undertaking), "In2Track3 – Research into optimised and future railway infrastructure" (funded by European funds through H2020, SHIFT2RAIL Innovation Programme), and Base Funding – UIBD/04708/2020 of the CONSTRUCT – Instituto de I&D em Estruturas e Construções – funded by national funds through FCT/MCTES (PIDDAC).

References

[1] CEN/TC 250, "N 3659 (Timeline for the evolution of the EN Eurocodes)," 2023.

[2] T. Arvidsson, A. Andersson, and R. Karoumi, "Train running safety on non-ballasted bridges," *International Journal of Rail Transportation*, vol. 7, pp. 1–22, 2018. [Online]. Available: https://doi.org/10.1080/23248378.2018.1503975

[3] G. Ferreira, P. Montenegro, A. Andersson, A. A. Henriques, R. Karoumi, and R. Calçada, "Critical analysis of the current Eurocode deck acceleration limit for evaluating running safety in ballastless railway bridges," *Engineering Structures*, vol. 312, p. 118127, Aug. 2024. [Online]. Available: https://www.sciencedirect.com/science/article/pii/S0141029624006898

[4] CEN, *Eurocode EN 1990: Basis of structural Design*. European Committee for Standardization, 2002.

[5] ERRI D 214/RP 8, "Rail bridges for speeds $>$ 200 km/h: Confirmation of values against experimental data," European Rail Research Institute, Utrecht, Tech. Rep., 1999.

[6] S. Schneider and S. Marx, "Design of railway bridges for dynamic loads due to high-speed traffic," *Engineering Structures*, vol. 174, pp. 396–406, Nov. 2018. [Online]. Available: https://www.sciencedirect.com/science/article/pii/S0141029618300580

[7] K. Matsuoka, A. Collina, C. Somaschini, and M. Sogabe, "Influence of local deck vibrations on the evaluation of the maximum acceleration of a steel-concrete composite bridge for a high-speed railway," *Engineering Structures*, vol. 200, p. 109736, Dec. 2019.

[8] Y. Chen, L. Jiang, Z. Lai, and J. Li, "A novel evaluation of train running safety on the HSR bridges under earthquakes based on the observed track deformation rate," *Engineering Structures*, vol. 275, p. 115260, Jan. 2023. [Online]. Available: https://www.sciencedirect.com/science/article/pii/S0141029622013360

[9] Z. Lai, L. Jiang, W. Zhou, J. Yu, Y. Zhang, X. Liu, and W. Zhou, "Lateral girder displacement effect on the safety and comfortability of the high-speed rail train operation," *Vehicle System Dynamics*, vol. 60, no. 9, pp. 3215–3239, Sep. 2022, publisher: Taylor & Francis _eprint: https://doi.org/10.1080/00423114.2021.1942507. [Online]. Available: https://doi.org/10.1080/00423114.2021.1942507

[10] TSI, "Technical specification for interoperability relating to the infrastructure subsystem of the trans-european high-speed rail system," *Official Journal of the European Union, Brussels*, 2008.

[11] EN 14363, *Railway applications - Testing and Simulation for the acceptance of running characteristics of railway vehicles - Running Behaviour and stationary tests*. Brussels: European Committee for Standarization (CEN), 2016.

[12] T. Arvidsson and A. Andersson, "Train–track–bridge interaction for non-ballasted railway bridges on high-speed lines," KTH Royal Institute of Technology, Stockholm, Tech. Rep. TRITA-BKN Report 165, 2017.

[13] ANSYS®, "Academic research," Canonsburg, PA, USA, 2018.

[14] CEN, *Eurocode EN 1991-2: Actions of structures - part 2: Traffic loads on bridges*. European Committee for Standardization, 2003.

[15] J. M. Goicolea, "Simplified Mechanical Description of AVE S-103 - ICE3 Velaro E High Speed Train," School of Civil Engineering, Technical University of Madrid–UPM, Tech. Rep., 2014.

[16] Y.-S. Lee and S.-H. Kim, "Structural analysis of 3D high-speed train–bridge interactions for simple train load models," *Vehicle System Dynamics*, vol. 48, no. 2, pp. 263–281, Feb. 2010, publisher: Taylor & Francis

_eprint: https://doi.org/10.1080/00423110902751912. [Online]. Available: https://doi.org/10.1080/00423110902751912

[17] H. Claus and W. Schiehlen, "Modeling and Simulation of Railway Bogie Structural Vibrations," *Vehicle System Dynamics*, vol. 29, no. sup1, pp. 538–552, Jan. 1998, publisher: Taylor & Francis _eprint: https://doi.org/10.1080/00423119808969585. [Online]. Available: https://doi.org/10.1080/00423119808969585

[18] W. Zhai, P. Liu, J. Lin, and K. Wang, "Experimental investigation on vibration behaviour of a CRH train at speed of 350 km/h," *International Journal of Rail Transportation*, vol. 3, no. 1, pp. 1–16, Jan. 2015, publisher: Taylor & Francis _eprint: https://doi.org/10.1080/23248378.2014.992819. [Online]. Available: https://doi.org/10.1080/23248378.2014.992819

[19] EN 13848-5, *Railway applications - Track - Track geometry quality - Part 5: Geometric quality assessment*. Brussels: European Committee for Standarization (CEN), 2005.

[20] P. Montenegro, S. Neves, R. Calçada, M. Tanabe, and M. Sogabe, "Wheel–rail contact formulation for analyzing the lateral train–structure dynamic interaction," *Computers & Structures*, vol. 152, pp. 200–214, 2015, publisher: Elsevier. [Online]. Available: https://www.sciencedirect.com/science/article/pii/S0045794915000139

[21] MATLAB®, "Academic research," Natick, MA, USA, 2018.